Functional Materials 17, No.3 (2010)

XPS and ESR spectroscopy of ZrO_2-Y_2O_3-Cr_2O_3 nanopowders

I.A.Yashchishyn, A.M.Korduban, V.V.Trachevskiy*, T.E.Konstantinova, I.A.Danilenko, G.K.Volkova, I.K.Nosolev*

Received May 7, 2010

O.Galkin Donetsk Institute for Physics and Engineering, National Academy of Sciences of Ukraine, 72 R.Luxembourg St., 83114 Donetsk, Ukraine
* G.Kurdyumov Institute for Metal Physics, National Academy of Sciences of Ukraine, 36 Vernadsky Blvd., 03003 Kyiv, Ukraine

Doped zirconia nanopowders of ZrO_2 + 3 mol. % Y_2O_3 + xCr_2O_3 (x = 0, 0.3, 0.75, 1.5, 2.9) compositions have been prepared by co-precipitation technique and studied using X-ray diffraction, X-ray photoelectron spectroscopy, and spin electron resonance. Introduction of chromium oxide to zirconia stabilized with yttrium results in a nonuniform dependence of crystallite size, monoclinic phase amount and specific surface area on chromium concentration. The joint analysis of structural and spectroscopic data suggests that the crystallite size increase is connected with competition between dopants and the increase in monoclinic phase amount is connected with Zr^{2+} substitution for Cr^{2+} in the crystal lattice of zirconia nanopowders.

Нанопорошки легированного диоксида циркония ZrO_2 + 3 mol. % Y_2O_3 + xCr_2O_3 (x = 0, 0.3, 0.75, 1.5, 2.9) получены методом совместного осаждения и изучены методами рентгеноструктурного анализа, рентгеновской фотоэлектронной спектроскопии и электронного парамагнитного резонанса. Введение оксида хрома в стабилизированный иттрием диоксид циркония приводит к немонотонному изменению размера частиц, количества моноклинной фазы и площади удельной поверхности в зависимости от концентрации примеси. Анализ спектроскопических и структурных данных позволяет сделать предположение о том, что увеличение размеров частиц вызвано конкуренцией легирующих добавок, а рост количества моноклинной фазы связан с замещением ионов Zr^{2+} на ионы Cr^{2+} в решетке диоксида циркония.

1. Introduction

Doped zirconia possess an outstanding combination of properties, namely, mechanical strength and fracture toughness, corrosion resistance, thermal and chemical stability, high ionic conductivity, transparency within a wide spectral range, stability to neutron flux. This material is applied in various fields as a functional and structural ceramics including biocompatible ceramics, as an electrolyte for SOFC, as a catalyst, in medicine, etc. Stabilization of high-temperature polymorphs of zirconia is achieved by adding suitable oversized cations, for example, Ca^{2+}, Mg^{2+}, Y^{3+}, Ce^{4+}. Over last years, an increased interest is paid in literature to multicomponent doping of zirconia with two or more elements providing the material properties to be varied in a wider range. [1-5]. Among many elements used for doping, chromium seems to be the least learned one, but in our opinion, it is one of the most interesting dopants, due to its smaller ionic radius (RCr = 0.063 nm, RZr = 0.084 nm), multivalence and possibility of identification by variety of spectroscopic techniques. Our previous works on chromium doping of stabilized zirconia [6, 7] show that this element produces a

significant impact on the ZrO_2-Y_2O_3 system properties. Those works have discovered several interesting effects, in particular, the elevation of nanopowder crystallization temperature, particle growth suppression, and a significant increase in the number of paramagnetic centers. Computer simulation of Cr impurity in ZrO_2 crystal [8] have shown a change in the electron structure of zirconia with chromium being a donor. Besides of the electron structure change, the presence of Cr ion in cation position of zirconia crystal increases the binding energy of OH groups with nanoparticles surface resulting in the inhibition of hydroxide/oxide transformation and shifting the crystallization temperature towards higher values. However, the above results were obtained for only two chromium concentrations (0.5 and 5 mol.% Cr_2O_3). Thus, in order to explore the influence of chromium doping on stabilized zirconia properties in more detail, a new set of samples was prepared consisting of five samples with chromium oxide concentrations in the range 0-3 mol. % and yttrium oxide 3 mol.%. The chromium oxide / yttrium oxide ratio has been chosen to be 0, 0.1, 0.25, 0.5 and 1.0. This work presents the investigation results of ZrO_2-Y_2O_3-Cr_2O_3 system using X-ray diffraction, XPS and ESR spectroscopy.

2. Experimental

The co-doped zirconia nanopowders were prepared by co-precipitation technique. The mixed water solutions of $ZrO(NO_3)_2$, $Y_2(NO_3)_3$ and $Cr(NO_3)_3$ taken at stoichiometric ratios were used as starting materials. The precipitates were dried at 120°C and calcined in air at 600°C for 2 h followed by natural cooling together with the furnace. The samples of following compositions were investigated: ZrO_2 + 3% mol. Y_2O_3 + x% Cr_2O_3, where x = 0, 0.3, 0.75, 1.5, 2.9. In what follows, the samples are referred to as ZYC_r with r being 0, 0.1, 0.25, 0.5, 1.0 and indicating the chromium oxide / yttrium oxide ratio. An X-ray diffractometer (XRD) with nickel-filtered Cu Kα radiation was used to determine the phase composition and crystallite size of calcined powder. The crystallite size was estimated using the Scherrer formula [9]. The phase composition was calculated from the intensities of the 111 and $\bar{1}11$ diffraction lines of m-ZrO_2 and 111 line of t-ZrO_2 [10]. The electron structure of nanopowders was investigated by X-ray photoelectron spectroscopy using an ES-2402 spectrometer (E MgK_α = 1253.6 eV, P = 200 W, $p = 2 \cdot 10^{-7}$ Pa) equipped with a PHOIBOS-100 SPECS energy analyzer. The spectrometer was also equipped with IQE-11/35 ion gun and FG-15/40 slow electron gun for compensation of surface charge of insulators. The XPS spectra were expanded using the Gauss-Newton method. The component areas were calculated after background subtraction by Shirley method. The ESR spectra were obtained using an ELEXIS 580 instrument at 9.8 GHz frequency. After integration, the initial ESR spectra were expanded into components using Gauss-Newton method.

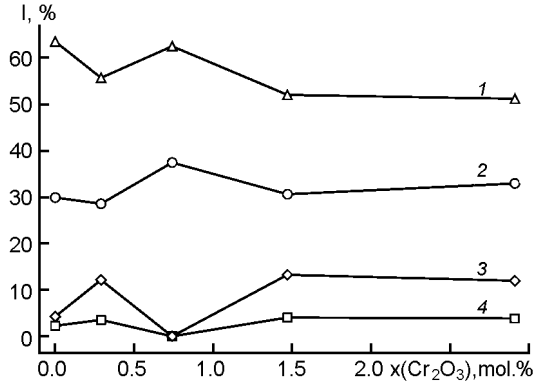

Fig. 1. Concentration dependences of Zr3d XPS spectrum. *1*– Zr^{4+}, *2* – Zr^{3+}, *3* – $Zr^{4+}(OH)$, *4* – Zr^{2+}.

3. Discussion

The X-ray diffraction shows that the crystallite size and phase composition of nanopowders vary nonmonotonously with

Table 1. Labels, chemical composition, average crystallite size (CSA) and specific surface area of investigated nanoparticles.

Label	Chemical composition	D (CSA), nm	m-phase, %	SBET, m^2/g
$ZYC_{0.0}$	ZrO_2 + 3 mol. % Y_2O_3	14.8	1.4	61.5
$ZYC_{0.1}$	ZrO_2 + 3.0 mol. % Y_2O_3 + 0.3 Cr_2O_3	17.6	4.0	48.3
$ZYC_{0.25}$	ZrO_2 + 3.0 mol. % Y_2O_3 + 0.75 Cr_2O_3	15.5	7.0	60.6
$ZYC_{0.5}$	ZrO_2 + 3.0 mol. % Y_2O_3 + 1.5 Cr_2O_3	14.5	4.5	69.0
$ZYC_{1.0}$	ZrO_2 + 3.0 mol. % Y_2O_3 + 2.9 Cr_2O_3	12.1	3.6	85.3

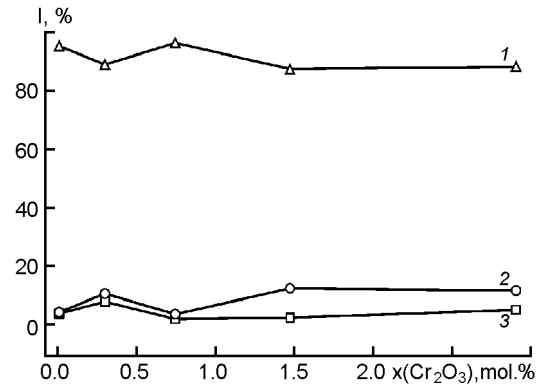

Fig. 2. Concentration dependences of O1s XPS spectrum. *1* – O^{2-}, *2* – (OH), *3* – $O^{(2+\delta)-}$.

chromium concentration increase and demonstrate maxima at particular chromium concentrations (Table 1.). The concentration dependence of specific surface area agrees well with that of crystallite size, showing that X-ray diffraction provides an adequate estimation of nanoparticle size. The maximum values of crystallite size and *m*-phase amount are attained at chromium oxide concentrations of 0.3 and 0.75 mol. %, respectively. The chromium introduction to yttrium stabilized zirconia results in a significant increase of crystallite size at 0.3 mol.% chromium oxide concentration followed by a monotonous decrease in crystallite size with increasing chromium fraction. Our previous work [11] shows that a significant segregation of yttrium takes place at this concentration; this is also supported by FTIR and NMR data of this system published in [12].

The decomposition results of Y3d and Cr2p XPS spectra are presented in Table 2 and concentration dependences of Zr3d and O1s spectra components are shown in Fig. 1 and Fig. 2, respectively. The decomposition of Zr3d spectra into components demonstrates the presence of zirconium ions in four nonequivalent states: main oxidation state Zr^{4+} (E_b = 182.0 eV), oxide states Zr^{3+} (E_b = 181.3 eV) and Zr^{2+} (E_b = 180.2 eV), and hydroxide state Zr^{4+}(OH) (E_b = 182.6 eV). The majority of surface zirconium ions are in main oxidation state Zr^{4+} (about 55%), approximately 30% of Zr ions, in Zr^{3+} and the remaining fraction is shared between hydroxide states and Zr^{2+} ones. The presence of Zr^{2+} is uncommon for that oxide, but it was observed by other researchers [13, 14] and connected with oxygen vacancies as well as the Zr^{3+} state. Concentration dependences of components intensities include two extreme points corresponding to maximum values of crystallite size and *m*-phase amount. The variation of hydroxide state amount with chromium concentration correlates well with oxide state variation and connected with OH group elimination from the nanoparticle surface.

The Y3d XPS spectrum comprises only two components corresponding to main oxide state Y^{3+} and yttrium ions connected with hydroxide groups. It should be mentioned that vast majority of yttrium ions are in the main oxide state (see Table 2.). The O1s spectrum decomposition reveals three main components: O^{2-} (E_b = 529.6 eV), $O^{(2+\delta)-}$ (E_b = 527-528 eV) and components with E_b = 531.2 and E_b = 531.7 eV corresponding to oxygen ions of surface hydroxyl groups of different type [15]. The $O^{(2+\delta)-}$ component can be attributed to oxygen ions with redundant electron density localized near oxygen vacancies, and its intensity corresponds to the amount of oxygen vacancies on the nanoparticle surface. The O^{2-} component dominating in all the spectra is attributed to main oxidation state of zirconium ions. Besides, the signals from yttrium and chromium oxides are present in the binding energy range E_b = 529.3 - 530.3 eV. The concentration dependences of three main components are shown in Fig. 2. It is to note as well that a significant increase of $O^{(2+\delta)-}$ component intensity at 0.3 mol.% concentration is connected with the yttrium

Table 2. Relative component intensities in Cr2p and Y3d XPS spectra.

Label	Relative intensities, %				
E_b, eV	Cr^{2+}, 575.5	Cr^{3+}, 576.5	Cr^{3+}(OH), 577.5	Cr^{5+}, 578.4	Y^{3+}, 156.7
$ZYC_{0.0}$	0	0	0	0	92.33
$ZYC_{0.1}$	24.99	33.41	39.47	2.14	83.87
$ZYC_{0.25}$	32.26	42.88	21.26	3.61	94.31
$ZYC_{0.5}$	11.39	40.45	42.14	6.02	93.18
$ZYC_{1.0}$	15.37	39.77	37.71	7.15	87.72

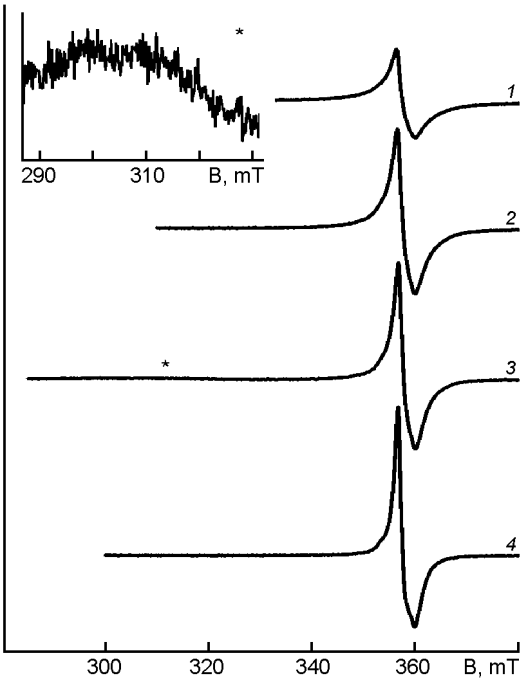

Fig. 3. ESR spectra of nanopowders. Inset: signal corresponding to clusters of exchange interacting paramagnetic ions Cr^{3+}(d3) and Cr^{2+}(d4). *1* – $ZYC_{1.0}$, *2* – $ZYC_{0.5}$, *3* – $ZYC_{0.25}$, *4* – $ZYC_{0.1}$.

surface segregation [11] and increasing amount of oxygen vacancies at the nanoparticle surface according to mechanism described in [17].

The decomposition of Cr2p spectrum into components shows chromium ions in four charge states at the nanoparticle surface. These states correspond to the main oxidation state of chromium oxide Cr^{3+}, Cr^{2+} and Cr^{5+} oxide states, and those corresponding to the Cr^{3+}(OH) ions connected with hydroxide groups. The distribution of component intensities as depending on chromium concentration is different (Table 2.) The minimum values of oxide and hydroxide Cr^{3+} states are attained at 0.75 mol.% chromium oxide concentration; the amount of Cr^{2+} states reaches its maximum at the same concentration along with the m-phase amount. The concentration dependence of Cr^{5+} state is monotonous and does not exceed 10% in intensity.

The parameters of ESR lines make it possible to assign the observed signals to paramagnetic Zr^{3+}, Cr^{3+} and Cr^{5+} ions. The component with g =1.958 corresponds to Cr^{5+}, that with g =1.951, to the signal of Cr^{3+} ions and the broad line with g =1.980 is attributed to Zr^{3+} ions. Besides of the

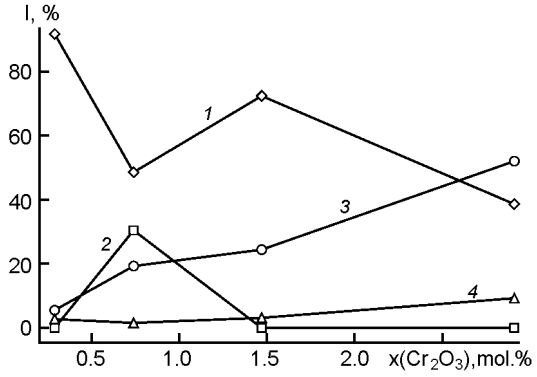

Fig. 4. Concentration dependences of paramagnetic centers obtained by ESR. *1* – Cr^{3+}, *2* – Cr^{3+}...Cr^{2+}, *3* – Zr^{3+}(OH), *4* – Cr^{5+}.

signals mentioned, an additional broad line with g = 2.236 is observed for the sample with 0.75 mol.% of chromium oxide and is attributed to the appearance of exchange interacting clusters of paramagnetic ions C^{3+}(d3) and Cr^{2+}(d4).

The joint analysis of spectroscopic data and X-ray diffraction results shows that for chromium concentrations of 0.3 and 0.75 mol. %, the properties of this system change considerably, in particular for the crystallite size and *m*-phase amount. A significant increase of crystallite size at chromium concentration of 0.3 mol. % is attributed to the competition of dopants during the particle growth with yttrium displacement to the nanoparticle surface [11] and can be connected with higher chromium electronegativity comparing to yttrium. The significant increase of *m*-phase amount at chromium concentration of 0.75 mol. % can be connected with the substitution of Zr^{2+} ions for Cr^{2+} ions in the nanoparticle crystal lattice and the system destabilization because of smaller ionic radius of the latter. These presumptions are supported by the concentration dependences of corresponding component intensities in the XPS spectra (Fig. 1, Table 2.), as well as by the appearing clusters of exchange interacting paramagnetic ions Cr^{3+}(d3) and Cr^{2+}(d4) evidenced by the ESR spectra [16]. According to [16], Zr^{2+} states play an important role in zirconia phase stabilization.

The lack of correlation between concentration dependences of paramagnetic Zr^{3+} centers between XPS and ESR data is connected with the fact that ESR data are attributed to bulk and surface centers and XPS data is limited only to the 2-3 nm thick surface layer. The amount of oxygen vacan-

cies at the nanoparticle surface agrees also with the above assumptions; the sharp increase of oxygen vacancies amount at the nanoparticle surface at chromium concentration of 0.3 mol. % corresponds to significant yttrium segregation to the nanoparticle surface while the further monotonous increase thereof corresponds to the increase of Cr^{3+} states amount according to the chemical composition and mechanism of oxygen vacancies appearance for described systems [17].

4. Conclusions

The doping of yttrium stabilized zirconia with chromium oxide in the mentioned range results in nonmonotonous changes in the structure and spectroscopic properties of the system. The significant changes of properties occur at chromium oxide concentrations of 0.3 and 0.75 mol.%, while the further concentration increase causes monotonous variation of the nanopowder properties. Basing on joint analysis, two assumptions are made: (i) the crystallite size increase is attributed to the competition between doping additives and accompanied by a significant segregation of yttrium to the nanoparticle surface; (ii) increase in *m*-phase amount is connected with the substitution of Zr^{2+} ions for Cr^{2+} ions in the zirconia lattice, resulting in a destabilization of the metastable tetragonal zirconium dioxide polymorph.

References

1. C. R. Foschini, D. P. F. Souza, P. I. Paulin Filho, et al., *J. Eur. Cer. Soc.* **21**, 1143 (2001).
2. Yanmei Kan, Guojun Zhang, Peiling Wang et. al., *J. Eur. Cer. Soc.* **26**, 3607 (2006).
3. Qiang Zhen, Ruifang Chen, Kai Van et al., *J. Rare Earths*, **25**, 199 (2007).
4. G. L. Markaryan, L. N. Ikryannikova, G. P. Muravieva et al, *Colloids and Surfaces A: Physicochem. Engin Aspects*, **151**, 435 (1999)
5. P. Ratnasamy, D. Srinivas, C. V. V. Satyanarayana et al., *J. Catalysis*, **221**, 455 (2004).
6. T.E. Konstantinova, V.V. Tokiy, I.A. Danilenko et al., *Nanosystems, Nanomaterials, Nanotechnologies*, **6**, 1147 (2008).
7. A.M. Korduban, I.A. Yashchishyn, T.E. Konstantinova et al., *Functional Materials* 14, 454 (2007).
8. N. Tokiy, T. Konstantinova, D. Savina et al., in: Proc. of Conf. CIMTEC' 2002 (Firenze), p. 127 (2002).
9. A. L. Patterson, *Phys. Rev.* 56, 978 (1939).
10. T. V. Chusovitina, Yu. S. Toropov, M. G. Tretnikova, Refractories and Industrial Ceramics **32**, 277 (1991).
11. I.A. Yashchishyn, A.M. Korduban, V.V. Trachevskiy et al., *Ap. Surf. Sci.*, **256**, 7175 (2010).
12. I.A. Yashchishyn, A.M. Korduban, V.V. Trachevskiy et al., *Phys. and Chem. Solid State*, **11**, 181 (2010).
13. C. Diagne, H. Idriss, K. Pearson et al., *Comp. Rend. Chim.*, **7**, 617 (2004).
14. R.H. French, S.J. Glass, F.S. Ohuchi et al., *Phys. Rev.*, **B 49**, 5133 (1994).
15. A.A. Tsyganenko, V.N. Filimonov, *J. Mol. Str.*, **19**, 579 (1973).
16. A. Cimino, D. Cordischi, S. Febraro et al., *J. Mol. Cat.*, **55**, 23 (1989)
17. M. Hartmanova, K. Putyera, D. Tunega et al., *Ferroelectrics*, **176**, 203 (1996)

РФС та ЕПР спектроскопія нанопорошків системи ZrO_2-Y_2O_3-Cr_2O_3

І.А.Ящишин, А.М.Кордубан, В.В.Трачевський, Т.Е.Константинова, І.А.Даниленко, Г.К.Волкова, І.К.Носолєв

Нанопорошки легованого діоксиду цирконію ZrO_2 + 3 mol. % Y_2O_3 + xCr_2O_3 (x = 0, 0.3, 0.75, 1.5, 2.9) одержано методом співосадження та досліджено методами рентгеноструктурного аналізу, рентгенівської фотоелектронної спектроскопії та електронного парамагнітного резонансу. Легування стабілізованого оксидом ітрію діоксиду цирконію оксидом хрому призводить до немонотонної зміни розміру частинок, кількості моноклінної фази та питомої поверхні в залежності від концентрації домішок. Аналіз спектроскопічних та структурних даних показав, що збільшення розміру частинок викликано конкуренцією легуючих домішок, а зростання кількості моноклінної фази пов'язано з заміщенням іонів Zr^{2+} на іони Cr^{2+} у гратці діоксиду цирконію.